Stochastic Ion Heating from Many Overlapping Laser Beams in Fusion Plasmas

P. Michel,[1] W. Rozmus,[2,1] E. A. Williams,[1] L. Divol,[1] R. L. Berger,[1] R. P. J. Town,[1] S. H. Glenzer,[1] and D. A. Callahan[1]

[1]*Lawrence Livermore National Laboratory, Livermore, California 94551, USA*
[2]*Theoretical Physics Institute, University of Alberta, Edmonton, Alberta T6G2G7, Canada*

In this Letter, we show through numerical simulations and analytical results that overlapping multiple (N) laser beams in plasmas can lead to strong stochastic ion heating from many ($\propto N^2$) electrostatic perturbations driven by beat waves between pairs of laser beams. For conditions typical of inertial-confinement-fusion experiment conditions, hundreds of such beat waves are driven in mm^3-scale plasmas, leading to ion heating rates of several keV/ns. This mechanism saturates cross-beam energy transfer, with a reduction of linear gains by a factor ~4–5 and can strongly modify the overall hydrodynamics evolution of such laser-plasma systems.

Experiments on large-scale laser facilities exploring high-energy-density physics or inertial confinement fusion (ICF) often require overlapping multiple intense ($> 10^{14}$ W/cm^2) laser beams in plasmas [1]. This leads to a wide range of new and complex multibeam laser-plasma interactions. A particularly important phenomenon is cross-beam energy transfer (CBET) [2], which was predicted to play a crucial role for indirect-drive experiments on the National Ignition Facility (NIF) [3] and has subsequently been used to advantage via laser wavelengths adjustments to tune the ICF targets' implosion symmetry [4–6]. On the other hand, for direct-drive experiments at the Omega facility, CBET tends to reduce the laser energy absorbed in the corona by transferring energy from the incoming light into the refracted outgoing light [7,8]. In such situations, the overlap of N laser beams generates $N(N − 1)/2$ individual beat waves whose phase velocities are fixed (determined by the laser beams' wavelengths and directions), and can be near the ion acoustic velocity due to either small wavelength adjustments as is done on NIF (cf. Fig. 1), or to sonic flows as in direct-drive or planar foil experiments [9]. Each beat wave drives an electrostatic potential via the ponderomotive force. The resulting density perturbation is driven resonantly if the beat wave's phase velocity matches the phase speed of an ion acoustic wave in the reference frame of the plasma. The scattering of laser light on these driven fluctuations transfers momentum and energy to the plasma: For each photon scattered from laser beam n to laser beam m, the momentum and energy transferred are, respectively, $\delta \boldsymbol{p} = \hbar(\boldsymbol{k}_n − \boldsymbol{k}_m)$ and $\delta U = \hbar(\omega_n − \omega_m)$, where $\omega_{m,n}$ and $\boldsymbol{k}_{m,n}$ are the photons' frequencies and wave vectors. Thus, overlapping many of these driven waves can directly affect the laser energy flux direction and the hydrodynamics evolution.

In this Letter, we show that the interactions of many beat waves with a plasma lead to strong stochastic heating of the ions. For typical indirect-drive ICF plasmas [10], we calculate ion-heating rates of several keV/ns. The acoustic

velocity is consequently increased by $\simeq 50\%$ in less than a nanosecond; the local hydrodynamics conditions in the laser beams' overlap region are thus largely dominated by the stochastic ion-heating mechanism, which takes place on time scales shorter than ion heat convection (due to plasma flow), ion conduction, and electron-ion temperature equilibration. This can in turn strongly modify the laser-plasma interaction mechanisms that take place in such regions, such as CBET. Using a particle code with binary collisions, we show that weak turbulence from the beat waves creates an energetic tail in the ion distribution function over time scales of a few ion bounce periods. Then, on time scales longer than the ion-ion collision time, collisions transfer the energy from the hot tail into the bulk; the distribution recovers a nearly Maxwellian shape, but with a rapidly increasing temperature and a change in average (flow) velocity. For NIF conditions,
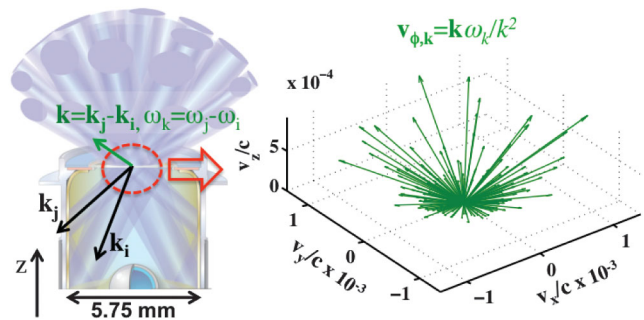

FIG. 1 (color). Upper half of a NIF hohlraum, where 96 of the 192 NIF laser beams, grouped in 24 quadruplets, overlap in a mm^3-scale plasma at the upper laser entrance hole (the lower half, not shown, has identical geometry), leading to 276 possible individual pairs. Each pair of quads (m, n) drives a beat wave with a phase velocity $\boldsymbol{v}_{\phi,k} = \boldsymbol{k}\omega_k/k^2$, where $\omega_k = \omega_n − \omega_m$ and $\boldsymbol{k} = \boldsymbol{k}_n − \boldsymbol{k}_m$. The beat waves' $\boldsymbol{v}_{\phi,k}$ are represented on the right (green arrows), for a wavelength separation between inner and outer beams of $\Delta\lambda = 2$ Å (with $\lambda_{\mathrm{out}} = 351$ nm and $\lambda_{\mathrm{inn}} = 351.2$ nm).

we calculate a reduction of CBET linear gains by a factor ~ 4–5. The process eventually stabilizes as the ion acoustic velocity becomes larger than the beat waves' phase velocities.

Our numerical model calculates the ion distribution function $f_i(\boldsymbol{r}, \boldsymbol{v}, t)$ by integrating equations of motion of particles in the presence of many beat waves and collisions; the space average of the resulting particle distribution function is then used to calculate the self-consistent evolution of the fields. Each beat wave between two lasers (m, n) with frequencies $\omega_{m,n}$ and wave vectors $\boldsymbol{k}_{m,n}$ creates a ponderomotive potential $\phi_{p,k} = \frac{1}{2}\hat{\phi}_{p,k}\exp[i\psi_k] + \text{c.c.}$ oscillating at the beat wave's phase, $\psi_k = \boldsymbol{k}\cdot\boldsymbol{r} - \omega_k t + \nu_k$, where $\omega_k = \omega_n - \omega_m$, $\boldsymbol{k} = \boldsymbol{k}_n - \boldsymbol{k}_m$, and ν_k is a random phase term between 0 and 2π which accounts for the fact that laser beams on large-scale facilities are optically smoothed and thus uncorrelated with one another. Beat waves from two laser beams with different frequencies ($\omega_k \neq 0$) have a finite phase velocity $\boldsymbol{v}_{\phi,k} = \boldsymbol{k}\omega_k/k^2$. The ponderomotive potential acts on the electrons to create a charge separation which results in an electrostatic potential $\phi_k = \frac{1}{2}\hat{\phi}_k\exp[i\psi_k] + \text{c.c.}$ which acts on both the electrons and the ions. The equations of motion for the ions are integrated with a Runge-Kutta method in the presence of many of these electrostatic potentials and with ion-ion collisions, $m_i d\boldsymbol{v}_i/dt = -q_i\sum_k\nabla\phi_k(\boldsymbol{r}, t) + \bar{C}_{\text{i-i}}$, where m_i and q_i are the ion mass and charge, and $\bar{C}_{\text{i-i}}$ is a binary ion-ion collision operator based on Ref. [11]. Here, we assume that the electrons' response is linear and that their averaged distribution remains Maxwellian with a constant temperature. As will be discussed later, only ion-ion collisions will be significant for ICF-relevant conditions; electron-ion thermal equilibration rates are typically too slow for the ions to affect the electron temperature.

The resulting ion distribution function is used to self-consistently calculate the evolution of the electrostatic potentials. The main assumption of the model is that these potentials have spatially uniform, slowly time-varying envelopes, $\hat{\phi}_k = \hat{\phi}_k(t)$, and follow the time evolution of the spatially averaged distribution function. Wave-wave couplings are neglected. In order to calculate the electrostatic potentials, the ion distribution is decomposed into its spatial average and the responses to the waves, $f_i(\boldsymbol{r}, \boldsymbol{v}, t) = f_{i0}(\boldsymbol{v}, t) + \sum_k\delta f_{ik}(\boldsymbol{r}, \boldsymbol{v}, t)$, where f_{i0} varies slowly compared to the fast oscillations of the beat waves. Poisson's equation connects each beat wave's electrostatic potential to the resulting density perturbation: $-\nabla^2\phi_k = 4\pi\sum_\alpha\int d^3v\,\delta f_{\alpha k}$, where α is the particle specie ($= e$ or i). Combining it with the Vlasov equation, $[\partial_t + \boldsymbol{v}\cdot\boldsymbol{\nabla} - (q_\alpha/m_\alpha)\sum_k\boldsymbol{\nabla}(\phi_k + \delta_{e\alpha}\phi_{p,k})\partial_{\boldsymbol{v}}]f_\alpha = 0$, where $\delta_{\alpha\alpha'}$ is a Kronecker delta, we get the expression for the electrostatic potential driven by the ponderomotive potential: $(1 + \chi_{ek} + \chi_{ik})\hat{\phi}_k = -\chi_{ek}\hat{\phi}_{p,k}$. For hot ICF plasmas ($\geq 1$ keV), the phase velocities are negligible compared to the electron thermal velocity, $v_{\phi,k} \ll v_{Te}$,

so the electron susceptibility is $\chi_{ek} \simeq 1/(k\lambda_{De})^2$. (Calculations with electrons showed no changes in their distribution function; in the following discussion, we will thus consider only the evolution of the ion distribution.) On the other hand, the fastest beat waves' phase velocities are larger than the ion thermal velocity. The ion susceptibility evolution follows the space-averaged ion distribution:

$$\chi_{ik}(t) = \frac{4\pi q_i^2}{k^2 m_i}\int \boldsymbol{k}\cdot\frac{\partial f_{i0}(\boldsymbol{v}, t)}{\partial\boldsymbol{v}}\frac{d^3v}{\omega - \boldsymbol{k}\cdot\boldsymbol{v}}. \quad (1)$$

The amplitudes of the electrostatic potentials thus follow the slowly varying space-averaged distribution function f_{i0}, with:

$$\phi_k(\boldsymbol{r}, t) = |\hat{\phi}_{p,k}|\frac{\chi_{ek}}{|1 + \chi_{ek} + \chi_{ik}(t)|}\cos[\psi_k(\boldsymbol{r}, t)]. \quad (2)$$

The integration in Eq. (1) is carried out numerically similarly to Ref. [12]. The ponderomotive potential $\phi_{p,k}$ created by two laser beams (m, n) with circular polarizations (or, equivalently, two NIF quadruplets with a "checkerboard" polarization arrangement, which behave like two temporally coherent but spatially incoherent beams [6]) crossing at an angle θ_{mn} is $|\hat{\phi}_{p,k}| = \frac{1}{4}(m_e c^2/e)a_m a_n(1 + \cos^2\theta_{mn})^{1/2}$, where $a = v_{\text{osc}}/c \approx 0.85(I_{18}\lambda_\mu^2)^{1/2}$ is the normalized laser vector potential. (I_{18} is the laser intensity in units of 10^{18} W/cm^2 and λ_μ is its wavelength in microns.) In the case of two beams with linear and parallel polarizations, we have $|\hat{\phi}_{p,k}| = \frac{1}{2}(m_e c^2/e)a_m a_n$.

We present calculations for the entrance hole of a NIF hohlraum, where 96 laser beams grouped in 24 quadruplets or "quads" cross, generating 276 beat waves overlapping in a mm^3-scale plasma (cf. Fig. 1). The quads are grouped in four cones propagating at 23.5° (4 quads), 30° (4 quads), 44.5° (8 quads), and 50° (8 quads) from the hohlraum axis; the "inner quads" (23.5° and 30°) have an average intensity of 5×10^{14} W/cm^2, and the "outer quads" (44.5° and 50°) are at 10^{15} W/cm^2. The initial electron and ion temperatures are 2.8 and 0.8 keV, respectively; the electron density is 3% of critical; and the plasma is He ($Z = 2$). These are typical conditions at the beginning of the main ("fourth") NIF laser pulse. The 128 beat waves between an inner and an outer quad have a finite phase velocity, set by a wavelength shift of 2 Å (at $\lambda_0 = 351$ nm) between inner and outer quads [3,4]. The 148 others, generated by pairs of quads with similar wavelengths, are stationary in the laboratory frame, $v_\phi = 0$. The ion-ion collision time is $\tau_{ii} \simeq 60$ ps. On the other hand, the thermal equilibration time for the electrons is $\tau^{e|i} \simeq 6$ ns [13]; this is too slow to be relevant for our conditions, which is why we consider only ion-ion collisions in our model.

The evolution of the ion distribution function is shown in Fig. 2 for typical NIF conditions. The 276 green dots represent the beat waves' phase velocities. Because of the NIF geometry, the problem is axisymmetric around z,
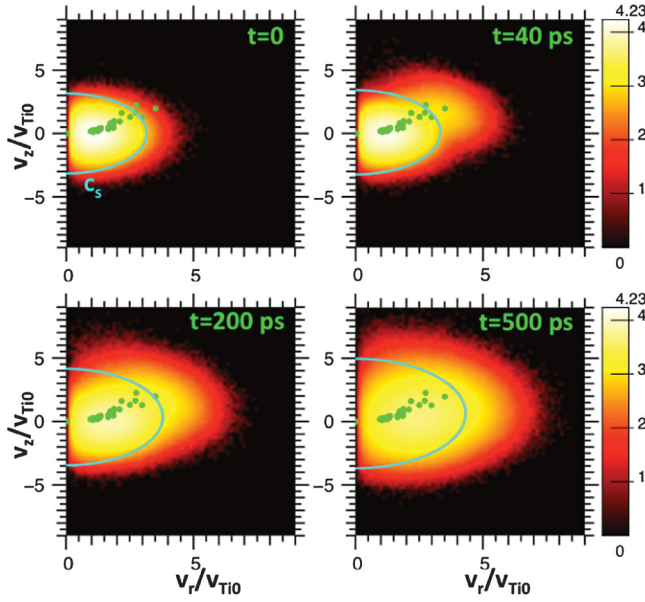
FIG. 2 (color). Ion velocity distribution function $\log[f_i(\boldsymbol{v})]$ from our particle code, plotted vs v_z and v_r (the distribution is axisymmetric along z) at times $t = 0$, 40, 200, and 500 ps. The cyan contour line represents the ion acoustic velocity c_s, and the green dots represent the 276 beat waves' phase velocities for the NIF geometry with $\Delta\lambda = 2$ Å. The initial plasma conditions are $T_e = 2.8$ keV, $T_i = 0.8$ keV, $n_e/n_c = 3\%$, and $Z = 2$ (He), and the laser intensities are 5×10^{14} and 10^{15} W/cm^2 for the "inner" and "outer" quads, respectively.

FIG. 3 (color). Time evolution of (a) ion temperature (defined as $k_B T_i = \frac{1}{3} m_i(\langle v^2 \rangle - \langle v \rangle^2)$), (b) average velocity, and (c) average exponential CBET spatial gain for a NIF inner beam. The black curves are the results from the particle code, and the dashed red curves are from the quasilinear reduced model.

the hohlraum axis (cf. Fig. 1). The ion distribution is initially Maxwellian at $t = 0$. The beat waves that have their phase velocities near the acoustic velocity c_s (cyan isocontour line) drive the strongest electrostatic perturbations. Overall, the initial electrostatic potentials' amplitudes $\hat{\phi}_k$ are in the range $[10^{-6}–10^{-5}] m_e c^2/e$, corresponding to density perturbations $\delta n/n \approx [10^{-4}–10^{-3}]$. The ion bounce periods τ_b are of a few ps.

In the early stages, for times smaller than the collision time ($t \lesssim \tau_{ii} \simeq 60$ ps), some potentials $\hat{\phi}_k(t)$ exhibit nonlinear oscillations at τ_b due to trapped particles, as described in Ref. [14]. However, after a few bounce periods, turbulence starts to dominate, diffusing particles between multiple overlapping resonances. The nonlinear oscillations disappear, and an energetic tail starts to develop in the ion distribution near the velocity of the fastest beat waves, around 3 to 4 times the initial ion thermal velocity v_{Ti0}, as shown in Fig. 2 at $t = 40$ ps. The total kinetic energy of the particles rapidly increases due to continuous injection of ions into the hot tail.

At later times, for $t \gg \tau_{ii}$, ion-ion collisions transfer the energy from the hot tail into the bulk, leading to an increase in ion temperature. After 200 ps, the bulk of ions has broadened and reached a thermal velocity close to the phase velocity of the fastest drivers; the tail that was present at $t = 40$ ps is now barely visible. At $t = 500$ ps,
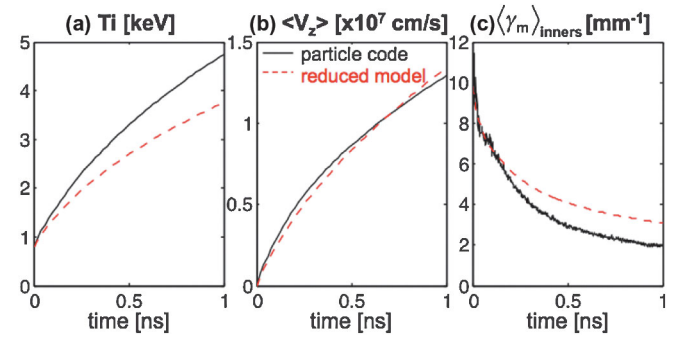
the distribution resembles a drifting Maxwellian with $\langle v_z \rangle \approx 0.6 v_{Ti0} = 0.85 \times 10^7$ cm/s.

The thermal energy of the particles and their average velocity are shown in Figs. 3(a) and 3(b). The ion temperature increases up to 4 keV in less than a nanosecond, and the particles acquire a drift $\langle v_z \rangle > 10^7$ cm/s due to momentum deposition [15,16]. The acoustic velocity $c_s = [(Z k_B T_e + 3 k_B T_i)/m_i]^{1/2}$ increases from 4.4×10^7 cm/s to 6.7×10^7 cm/s in 1 ns.

Such ion heating rates are in qualitative agreement with simple estimates based on the conservation of action [17] during the CBET process, using experimental measurements. Typically, symmetric implosions on NIF for 420 TW shots require transferring 100–150 TW between laser beams in a $\simeq$ mm^3-size plasma near the hohlraum's laser entrance holes [18]. The power density deposited into plasma waves is therefore [100–150] TW $\times \delta\lambda/\lambda_0 \simeq 60$ to 120 GW/mm^3 for wavelength separations between laser beams of 2–3 Å (and $\lambda_0 = 351$ nm). Assuming an average ion density $n_i = 1.35 \times 10^{20}$ cm^{-3}, and that all the waves' energy eventually gets converted into heat, we get ion heating rates of ~2–5 keV/ns.

Calculations with an initial flow velocity at $t = 0$ (i.e., where the distribution at $t = 0$ in Fig. 2 would be centered around $2v_{Ti0}$, slightly below Mach 1, as is the case at the entrance hole of NIF hohlraums) show similar heating rates and tend to equilibrate at similar averaged velocities, near the velocity of the fastest beat waves (near $2v_{Ti0}$ in our case). Indeed, the flow energy $U_{\text{flow}} = \frac{1}{2} m_i \langle v_z \rangle^2$ deposited in the plasma via momentum deposition remains small compared to the thermal energy gained by the system (+ 0.4 keV vs +3 keV from 0 to 1 ns in our case). Also, note that, since the volume where all the beams overlap is of the order of a mm^3, the flow (similar to a Mach 1 nozzle flow near the entrance hole) will replace the ion population in that volume in 2–3 ns; therefore, calculations on times scales ≤ 1 ns should not be affected by changes in background conditions.

The effect of ion heating on CBET is represented in Fig. 3(c), which shows the average of the spatial gain exponent over the NIF "inner quad." The gain γ_m for a quad m (such that $\partial_z a_m^2 = \gamma_m a_m^2$) is defined using the convective growth formula [4,15],

$$\gamma_m = \sum_{n=1}^{24} \frac{-\chi_{ek}^2 \text{Im}(\chi_{ik})}{|1 + \chi_{ek} + \chi_{ik}|^2} \frac{k^2 a_n^2}{16 k_m} [1 + \cos^2(\theta_{mn})], \quad (3)$$

where $\boldsymbol{k} = \boldsymbol{k}_n - \boldsymbol{k}_m$ and the summation is taken over the 23 beat waves between the quad m and every other quad $n \neq m$. The gain drops by a factor ~ 4–5, which could help explain the observed saturation of CBET in both direct- and indirect-drive experiments, where cumulative amplification from multiple laser beams over large scale lengths allows large gains even in the presence of very low levels of density fluctuations [7,19,20].

The heating rate eventually drops: The temperature increases up to the point where the acoustic velocity reaches the largest beat waves' phase velocities (soon after $t = 200$ ps, per Fig. 2). From then on, the ion acoustic resonance will be moved further away from the beat waves' fixed phase velocities, which will reduce their coupling to the plasma and thus slow the ion heating. This also means that the plasma will evolve into a regime where the electrostatic responses are essentially linear, as the beat waves' frequencies are not resonant with ion acoustic modes anymore.

Since collisions tend to rapidly thermalize the hot ion tail and restore a Maxwellian shape for the distribution function, we can derive a reduced model based on the assumption that the ions are described by a local Maxwellian with a time-varying temperature and average velocity. The distribution evolution follows quasilinear theory [21]: $\partial_t f_0(\boldsymbol{v}, t) = \partial_{\boldsymbol{v}} \cdot \bar{D} \cdot \partial_{\boldsymbol{v}} f_0(\boldsymbol{v}, t)$, with the diffusion operator:

$$\bar{D} = \frac{q_i^2}{2m_i^2} \sum_k |\hat{\phi}_k|^2 \boldsymbol{k}\boldsymbol{k} \,\text{Im} \frac{1}{\omega_k - \boldsymbol{k} \cdot \boldsymbol{v}}. \quad (4)$$

By taking the moments of f_{i0}, one can calculate the average flow and thermal energy, $\langle \boldsymbol{v} \rangle = n_i^{-1} \int d^3 v \, \boldsymbol{v} f_{i0}(\boldsymbol{v}, t)$ and $k_B T_i = \frac{1}{3} m_i (\langle v^2 \rangle - \langle v \rangle^2)$. Both are coupled via the time-varying ion susceptibility χ_i, so we get the following system of coupled equations:

$$\frac{d\langle \boldsymbol{v} \rangle}{dt} = \frac{-1}{8\pi m_i n_i} \sum_k |\hat{\phi}_k|^2 k^2 \text{Im}(\chi_{ik}) \boldsymbol{k}, \quad (5)$$

$$\frac{dk_B T_i}{dt} = \frac{1}{12\pi n_i} \sum_k |\hat{\phi}_k|^2 k^2 (\omega_k - \boldsymbol{k} \cdot \langle \boldsymbol{v} \rangle) \text{Im}(\chi_{ik}), \quad (6)$$

$$\chi_{ik}(t) = \frac{-\omega_{pi}^2 m_i}{2k^2 k_B T_i} Z'\left[\frac{\omega_k - \boldsymbol{k} \cdot \langle \boldsymbol{v} \rangle}{k\sqrt{2k_B T_i/m_i}}\right], \quad (7)$$

where Z' is the plasma dispersion function. Equation (5) is similar to Ref. [15] if ϕ_{pk} is estimated for the case of laser beams with the same polarization.

The total energy of the ions $U_{\text{tot}} = \frac{1}{2} m_i \langle v^2 \rangle$ is distributed between thermal and flow energy, $U_{\text{tot}} = \frac{3}{2} k_B T_i + U_{\text{flow}}$, where $U_{\text{flow}} = \frac{1}{2} m_i \langle v \rangle^2$. Note that, for beat waves produced by lasers with identical frequency, i.e., $\omega_k = 0$, there is no net transfer of energy to the plasma since $dU_{\text{tot}}/dt = 0$ per Eqs. (5) and (6); there is, however, a redistribution of the total energy of the ions from flow energy to heat. The implication is that, even for configurations where all the laser beams have the same wavelength, if beams cross in a flowing plasma, they will not only exchange energy [9] but will also reduce the plasma flow and increase the ion temperature.

This reduced model is compared to our particle code in Fig. 3. Because ion-ion collisions thermalize the distribution quickly enough, the reduced model reproduces the code's result to better than 20% for the temperature, and to a few % for the momentum. The disagreement for T_i comes from the fact that the distribution from the particle code still maintains a slight tail even at later times when $t \gg \tau_{ii}$. The agreement is better for the momentum, which is only the first-order moment of f_{i0} and is less sensitive to variations in the detailed shape of the distribution function. This model could in principle be included in hydrodynamics codes, allowing an improved and self-consistent description of hydrodynamics and laser-plasma interactions in regions where multiple laser beams overlap.

In conclusion, we have shown that strong ion heating can occur when multiple laser beams overlap in plasmas. The numerous beat waves between pairs of crossing laser beams drive electrostatic perturbations that transfer energy and momentum to the ions, leading to stochastic heating and plasma drift. For typical NIF conditions, the ion temperature increases at rates of several keV/ns, making stochastic heating a dominant mechanism for the hydrodynamics evolution of the plasma in the laser beams' overlap region, with heating rates being faster than ion temperature convection and conduction and electron-ion temperature equilibration. This results in the saturation of cross-beam energy transfer; linear gain exponents for NIF's inner beams drop by a factor ~ 4–5 in a nanosecond due to the increase in the ion acoustic velocity, which decouples the beat waves from ion acoustic modes. A quasilinear model is shown to reproduce the main observables from the particle code. The heating rate eventually slows as the electrostatic responses are driven further away from ion acoustic resonance. The changes in hydrodynamics conditions at the entrance holes of NIF targets from stochastic ion heating could also affect other laser-plasma interaction processes occurring in such regions, such as the reamplification of backscatter light by multiple incoming laser beams crossing the backscatter wave on its way out of the target [22]. One could also envision using controlled CBET to locally heat the plasma and mitigate other laser-plasma interaction processes.

[1] J. D. Lindl, P. Amendt, R. L. Berger, S. G. Glendinning, S. H. Glenzer, S. W. Haan, R. L. Kauffman, O. L. Landen, and L. J. Suter, Phys. Plasmas **11**, 339 (2004); N. Fleurot, C. Cavailler, and J. L. Bourgade, Fusion Eng. Des. **74**, 147 (2005); R. L. McCrory, D. D. Meyerhofer, R. Betti, R. S. Craxton, J. A. Delettrez, D. H. Edgell, V. Y. Glebov, V. N. Goncharov, D. R. Harding, D. W. Jacobs-Perkins *et al.*, Phys. Plasmas **15**, 055503 (2008).

[2] W. L. Kruer, S. C. Wilks, B. B. Afeyan, and R. K. Kirkwood, Phys. Plasmas **3**, 382 (1996); V. V. Eliseev, W. Rozmus, V. T. Tikhonchuk, and C. E. Capjack, *ibid.* **3**, 2215 (1996).

[3] P. Michel, L. Divol, E. A. Williams, S. Weber, C. A. Thomas, D. A. Callahan, S. W. Haan, J. D. Salmonson, S. Dixit, D. E. Hinkel *et al.*, Phys. Rev. Lett. **102**, 025004 (2009).

[4] P. Michel, S. H. Glenzer, L. Divol, D. K. Bradley, D. Callahan, S. Dixit, S. Glenn, D. Hinkel, R. K. Kirkwood, J. L. Kline *et al.*, Phys. Plasmas **17**, 056305 (2010).

[5] S. H. Glenzer, B. J. MacGowan, P. Michel, N. B. Meezan, L. J. Suter, S. N. Dixit, J. L. Kline, G. A. Kyrala, D. K. Bradley, D. A. Callahan *et al.*, Science **327**, 1228 (2010); J. D. Moody, P. Michel, L. Divol, R. L. Berger, E. Bond, D. K. Bradley, D. A. Callahan, E. L. Dewald, S. Dixit, M. J. Edwards *et al.*, Nat. Phys. **8**, 344 (2012).

[6] N. B. Meezan, L. J. Atherton, D. A. Callahan, E. L. Dewald, S. Dixit, E. G. Dzenitis, M. J. Edwards, C. A. Haynam, D. E. Hinkel, O. S. Jones *et al.*, Phys. Plasmas **17**, 056304 (2010); **17**, 109901 (2010)

[7] I. V. Igumenshchev, W. Seka, D. H. Edgell, D. T. Michel, D. H. Froula, V. N. Goncharov, R. S. Craxton, L. Divol, R. Epstein, R. Follett *et al.*, Phys. Plasmas **19**, 056314 (2012).

[8] D. H. Froula, I. V. Igumenshchev, D. T. Michel, D. H. Edgell, R. Follett, V. Y. Glebov, V. N. Goncharov, J. Kwiatkowski, F. J. Marshall, P. B. Radha *et al.*, Phys. Rev. Lett. **108**, 125003 (2012).

[9] K. B. Wharton, R. K. Kirkwood, S. H. Glenzer, K. G. Estabrook, B. B. Afeyan, B. I. Cohen, J. D. Moody, and C. Joshi, Phys. Rev. Lett. **81**, 2248 (1998).

[10] D. A. Callahan, N. B. Meezan, S. H. Glenzer, A. J. MacKinnon, L. R. Benedetti, D. K. Bradley, J. R. Celeste, P. M. Celliers, S. N. Dixit, T. Döppner *et al.*, Phys. Plasmas **19**, 056305 (2012); S. H. Glenzer, D. A. Callahan, A. J. MacKinnon, J. L. Kline, G. Grim, E. T. Alger, R. L. Berger, L. A. Bernstein, R. Betti, D. L. Bleuel *et al.*, Phys. Plasmas **19**, 056318 (2012).

[11] T. Takizuka and H. Abe, J. Comput. Phys. **25**, 205 (1977).

[12] J. P. Palastro, J. S. Ross, B. Pollock, L. Divol, D. H. Froula, and S. H. Glenzer, Phys. Rev. E **81**, 036411 (2010).

[13] J. D. Huba, *NRL Plasma Formulary* (Naval Research Laboratory, Washington, D.C., 2006) [http://wwwppd.nrl.navy.mil/nrlformulary/NRL_FORMULARY_06a.pdf].

[14] T. O'Neil, Phys. Fluids **8**, 2255 (1965).

[15] E. A. Williams, B. I. Cohen, L. Divol, M. R. Dorr, J. A. Hittinger, D. E. Hinkel, A. B. Langdon, R. K. Kirkwood, D. H. Froula, and S. H. Glenzer, Phys. Plasmas **11**, 231 (2004).

[16] H. A. Rose, Phys. Plasmas **3**, 1709 (1996).

[17] J. Manley and H. Rowe, Proc. IREE Aust. **44**, 904 (1956).

[18] R. P. J. Town, M. D. Rosen, P. A. Michel, L. Divol, J. D. Moody, G. A. Kyrala, M. B. Schneider, J. L. Kline, C. A. Thomas, J. L. Milovich *et al.*, Phys. Plasmas **18**, 056302 (2011).

[19] I. V. Igumenshchev, D. H. Edgell, V. N. Goncharov, J. A. Delettrez, A. V. Maximov, J. F. Myatt, W. Seka, A. Shvydky, S. Skupsky, and C. Stoeckl, Phys. Plasmas **17**, 122708 (2010).

[20] P. Michel, L. Divol, R. P. J. Town, M. D. Rosen, D. A. Callahan, N. B. Meezan, M. B. Schneider, G. A. Kyrala, J. D. Moody, E. L. Dewald *et al.*, Phys. Rev. E **83**, 046409 (2011).

[21] W. E. Drummond and D. Pines, Nucl. Fusion, Suppl. Part 3, 1049 (1962); A. A. Vedenov, E. P. Velikhov, and R. Z. Sagdeev, Nucl. Fusion **1**, 82 (1961); I. B. Bernstein and F. Engelmann, Phys. Fluids **9**, 937 (1966).

[22] R. K. Kirkwood, P. Michel, R. London, J. D. Moody, E. Dewald, L. Yin, J. Kline, D. Hinkel, D. Callahan, N. Meezan *et al.*, Phys. Plasmas **18**, 056311 (2011).